Online Monitoring of the Evolution of the Number of Particles in Emulsion Polymerization by Conductivity Measurements. I. Model Formulation

A. F. Santos,[1,2] E. L. Lima,[1] J. C. Pinto,[1] C. Graillat,[2] T. McKenna[2]

[1]*Programa de Engenharia Química, Coordenação dos Programas de Pós-Graduação em Engenharia, Universidade Federal do Rio de Janeiro, Cidade Universitária, CP 68502, Rio de Janeiro 21945-970 RJ, Brazil*

[2]*Centre National de la Recherche Scientifique-Laboratoire de Chimie et Procédé de Polymérisation, École Supérieure Chimie Physique Electronique de Lyon, Université Claude Bernard Lyon 1, 43 Blvd. du 11 Novembre 1918, Bât. 308F, 69616 Villeurbanne Cedex, France*

Received 19 July 2002; accepted 2 December 2002

ABSTRACT: A conductivity meter is an inexpensive instrument that can easily be installed in polymerization reactors. This instrument can be used to monitor ionic species without time-consuming calibrations. A probe is inserted into the media, providing *in situ* measurements of conductivity in real time. For emulsion polymerization reactions, the conductivity meter can respond to changes in the ionic surfactant concentration, allowing the determination of surfactant dynamics in the media. The surfactant concentration can then be related to the changes in the surface area of the polymer particle phase, which can be linked to nucleation or coagulation phenomena. In this study, a conductivity meter was coupled to a calorimetric reactor to provide *in situ* and online measurements of conductivity during the emulsion polymerization of styrene, with sodium dodecyl sulfate as an anionic surfactant and with potassium persulfate as a free-radical initiator. A semiempirical model was built to describe the conductivity signal as a function of the latex composition and the reactor temperature. The model was inverted and combined with the available conductivity signal, conversion, and temperature measurements and was able to accurately predict the number of polymer particles in the latex and the surfactant concentrations in the many phases, without online measurements of the particle size. J Appl Polym Sci 90: 1213–1226, 2003

Key words: emulsion polymerization; modeling; particle nucleation

INTRODUCTION

In an emulsion polymerization reactor, particle nucleation and the evolution of the particle size distribution are strongly related to the surfactant type and concentration.[1] In most processes, information on particle nucleation and the evolution of the number and size of particles is found essentially through offline measurements of the particle size distribution of samples taken from the reactor.[2] However, for the purpose of control, for which the online process monitoring of particle nucleation phenomena is required, this is not a satisfactory approach.[3]

A relatively inexpensive instrument that can easily be installed in polymerization reactors is the conductivity meter. This instrument can be used to monitor the mobility of ionic species without time-consuming calibrations. A probe can be inserted into the reaction medium to provide *in situ* measurements of conductivity in real time.[4] For emulsion polymerization reactions, the conductivity cell can respond to changes in the ionic surfactant concentrations, allowing the determination of surfactant dynamics in the media, which can be related to particle nucleation and/or coagulation phenomena. Additionally, conductivity measurements can also give insights about the emulsion polymerization kinetics.

Both the formation of particles (interval I according to the classical theory of emulsion polymerization) and the growth of particles (interval II) cause an increase in the total particle surface. In interval III, the particles tend to shrink as the monomer in the swollen particles is converted into denser polymer. Surfactant molecules present in the reactor are adsorbed from the aqueous phase onto the polymer particle surface, and this ensures the stability of the polymer latex. If ionic stabilization is employed, the surfactant molecules lose mobility after adsorption, and this leads to a decrease in the conductivity.[5]

Correspondence to: T. McKenna (mckenna@cpe.fr).

Contract grant sponsor: Brazil–France Cooperation CAPES/COFECUB; contract grant number: 236/98-II.

Contract grant sponsor: Fundação de Amparo à Pesquisa do Estado do Rio de Janeiro.

Contract grant sponsor: Conselho Nacional de Desenvolvimento Científico e Tecnológico.

In the last 10 years, some efforts toward the use of online conductivity measurement devices during polymerization processes have been made.[5–7] Janssen[5] performed online conductivity measurements during styrene (STY) emulsion and methyl methacrylate (MMA) emulsion polymerization reactions. The measurements were used for the better understanding of the course of the reactions. Sodium dodecyl sulfate (SDS) feed profiles were designed to reduce particle agglomeration on the basis of conductivity data, but only one experiment was carried out. The author showed that particle coagulation could be detected by the conductivity signal. The experimental results were interpreted under the assumption that the conductivity signal was composed of three distinct contributions: (1) the mobility of free surfactant molecules, (2) the mobility of surfactant micelles, and (3) the mobility of initiator ions in the aqueous phase.

Fontenot and Schork[6] used a recirculation loop with an inline probe for measurements of conductivity during miniemulsion and conventional emulsion (or macroemulsion) polymerizations. Although some inhibition caused by the silicone tubing used in the loop was observed during the reactions, the authors concluded that the method worked well and could be used to provide useful information about the different kinetic mechanisms in macroemulsions and miniemulsions. In particular, it was shown that the technique could provide a reliable indication of the end of interval II in macroemulsion polymerizations.

Reimers and Shork[7] used online conductivity measurements to study particle nucleation mechanisms during MMA miniemulsion polymerization. A conductivity cell was employed, with samples of the reaction mixture being fed into it via a positive-displacement pump. Readings from the cell were taken every 2 min, and the different intervals of the miniemulsion polymerizations were identified with the conductance measurements. A comparison with conventional emulsion process was made. It was observed that the conductivity curve was subject to smaller changes during the miniemulsion process, and this supported the idea that miniemulsion polymerizations could occur with little change in the surface characteristics.

In the aforementioned studies, the use of online conductivity data was limited to the qualitative description of emulsion polymerization processes and to the identification of kinetic intervals. No attempts were made to treat the conductivity signal quantitatively; the online monitoring and control of the emulsion polymerization reactions were the goals. According to Noel et al.,[8] the exact nature of all the factors that determine the conductivity signal is not totally clear yet.

In the work described in this article, a conductivity meter was coupled to a calorimetric reactor to provide *in situ* and online measurements of conductivity during the emulsion polymerization of STY, with SDS as an anionic surfactant and with potassium persulfate (KPS) as a free-radical initiator. Reactor and jacket temperatures were stored for offline energy balance calculations. A semiempirical model was then built to describe the conductivity signal as a function of the latex composition and reactor temperature. The model was able to provide useful information about the surfactant dynamics and allowed us to predict the number of polymer particles in the latex (N_p) without the need of online measurements of the particle size. It is believed that this type of model and measurement can be very useful for the development and implementation of interesting control applications.

EXPERIMENTAL

An experimental study was conducted to evaluate the effects of the latex composition on the conductivity signal. Several STY (>99%; Acros, France) emulsion polymerization reactions were carried out at different surfactant concentrations (SDS; >99%; Acros) with KPS (>99%; Acros) as an initiator.

The calorimetric reactor consisted of a 3-L jacketed glass reactor equipped with a valve at the bottom to enable the collection of latex samples. The reactor vessel and lid were jacketed with feed water at a constant temperature of 60°C. A condenser was used to minimize the loss of reactants, especially the monomer, through evaporation. Platinum resistance probes (PT100; precision = 0.1°C) were used to measure water inlet and outlet temperatures. The reactor temperature was measured by the insertion of a high-precision probe into the agitator axis. There were four inlets in the vessel wall to allow for the insertion of sensors into the reaction mixture. One of these holes was used to take conductivity measurements with a platinum cell. The three temperature measurements and the conductivity signal, via a conductivity meter (CD 810, Tacussel), were recorded by means of a data acquisition unit (HP 34970A).

The platinum sensor connected to the conductivity meter was inserted into the reactor to provide *in situ* measurements of the latex conductivity. Both the temperature and conductivity were measured every 10 s. Samples were regularly collected during the reaction for offline analysis of the conversion (gravimetry) and the average particle diameter (d_p) by dynamic laser light scattering (S7032, Malvern Instruments). This information was then used to calculate N_p, the latex surface area [S_L (cm^2)], and the surface coverage by the surfactant [θ (%)], which was dependent on the specific adsorption coverage area of the surfactant on the polymer particle (a_s). A number of researchers have investigated the adsorption phenomena of SDS on the polystyrene particle surface, and several values of a_s are reported in the literature (Table I). On the basis of

TABLE I
a_s Values of SDS over Polystyrene

T_r (°C)	a_s (Å^2)	Reference
20	44.0	11
20	40.0	13
20	49.3	16
22	47.1	20

the results presented in Table I, a_s is assumed to be equal to 45 (Å^2).

The standard recipe used for the polymerization runs contained 1620 g of distilled and deionized water (adjusted to keep 1820.0 g of the emulsion in the initial charge), 182 g of STY, and 1.82 g of KPS (initiator). All reactions were performed with a 10% solid content. The amount of SDS (surfactant) was changed in accordance with the individual experimental recipe over an interval of concentrations ranging from 0.7 to 5 times the critical micelle concentration (cmc).

Emulsion polymerization runs were carried out at different surfactant concentrations. In most experiments, water was initially charged to the reactor. For the removal of oxygen, the water was purged with nitrogen at a low flow rate for 5 min. The medium was stirred throughout the process at about 200 rpm. A surfactant was added to the reactor in two steps. When the reactor temperature reached 40°C, a fraction of the surfactant was added, and the reactor was then heated to 60°C. The remaining surfactant was then introduced to obtain the desired concentration in the reactor. The two-step addition procedure was used for calibration and fine tuning of the conductivity signal before the formation of the emulsion. Afterward, the monomer was added and was normally followed by a drop of the reactor temperature. The nitrogen purge was kept at low flow rates to minimize monomer evaporation. Finally, after the stabilization of the temperature and conductivity readings, the initiator (dissolved in a small quantity of water) was added, and the chronometer was started. The conductivity and temperatures were measured every 10 s during the entire procedure.

CONDUCTIVITY MEASUREMENTS IN WATER

Determination of the cmc of sds

The cmc can be defined as the concentration of the surfactant (g/L) above which an increase in the surfactant concentration leads to the appearance of micelles.[10] Conductivity measurements can be used to determine the cmc of an ionic surfactant because the conductance of an ion in solution is a function of both its charge and size (or mobility)[11,12] Equation (1) can be used to describe the total conductivity [σ (S/cm)] of a solution of SDS (or any ionic surfactant) in water:

$$\sigma = \sigma_0 + \Lambda_0^{Na^+}[Na^+] + \Lambda_0^{DS^-}[DS^-] \quad (1)$$

where Λ_0^{Na+} is the equivalent ionic conductivity at infinite dilution of the sodium ion (cm^2 S/mol), Λ_0^{DS-} is the equivalent ionic conductivity at infinite dilution of the dodecyl sulfate ion (cm^2 S/mol), [Na^+] is the concentration of the sodium ion (mol/cm^3), [DS^-] is the concentration of the dodecyl sulfate ion (mol/cm^3), and σ_0 is the conductivity contribution from all other ions present in the water (S/cm).

When SDS is slowly added into pure water, the conductivity increases until the cmc is reached. From this point onward, dodecyl sulfate molecules start to form micelles. Because of the larger aggregate size and lower mobility of the micelles, the rate of change of the conductivity signal changes above the cmc. A plot of the conductivity signal with increasing surfactant concentrations at a constant temperature produces two straight lines at the cmc.

Conductimetric titrations were carried out to determine the cmc of SDS in the aqueous medium at 25 and 60°C. Replicates were performed to ensure reproducibility. Average conductivity results are displayed in Figure 1. At 25°C, the experimental cmc is around 2.4 g/L, whereas the experimental cmc value increases to 3.0 g/L at 60°C. It must be pointed out that the measurement of the cmc of SDS is a controversial issue. As shown in Table II, several values have been reported in the literature, ranging from 1.7 to 2.5 g/L at ambient temperatures, although most are very close to 2.2–2.4 g/L. This seems to be related both to the purity of the SDS employed and to the technique applied for cmc characterization. Dodecyl alcohol and inorganic salts are among the impurities commonly encountered in commercial SDS samples. Such impurities are more surface-active than pure SDS, contributing to the de-

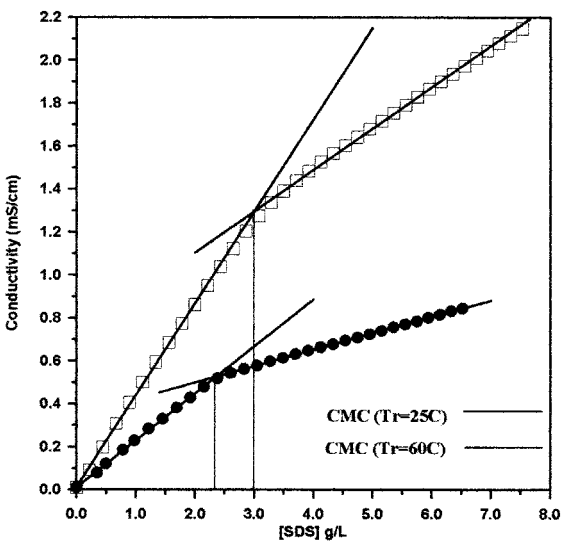

Figure 1 Conductimetric titrations of SDS in aqueous media at (●) 25 and (□) 60°C.

TABLE II
cmc Values for SDS at Different Temperatures and with Different Measurement Techniques

Temperature (°C)	cmc (g/L)	Method	Reference
20	2.43	Conductimetry	11
20	2.20	Conductimetry	13
25	2.3	Potentiometry	14
25	1.73	Tensiometry	15
25	2.4	Tensiometry	17
25	2.28	Dielectrometry	18
25	2.37	Conductimetry	18
25	2.31	Conductimetry	19
25	2.4	Conductimetry	This work
60	2.93	Conductimetry	5
60	3.0	Conductimetry	This work

crease of the cmc. Our values reported here, however, are in very good agreement with other cmc values obtained through conductivity measurements.

Effect of the temperature on the conductivity

Because the conductivity is influenced by the temperature, it is necessary to determine the relationship between these two variables. This is especially important in polymerization reactions, in which temperature variations are expected to occur. Figure 2 illustrates the evolution of the conductivity signal during the heating of different aqueous SDS solutions. The conductivity increases linearly with temperature, and

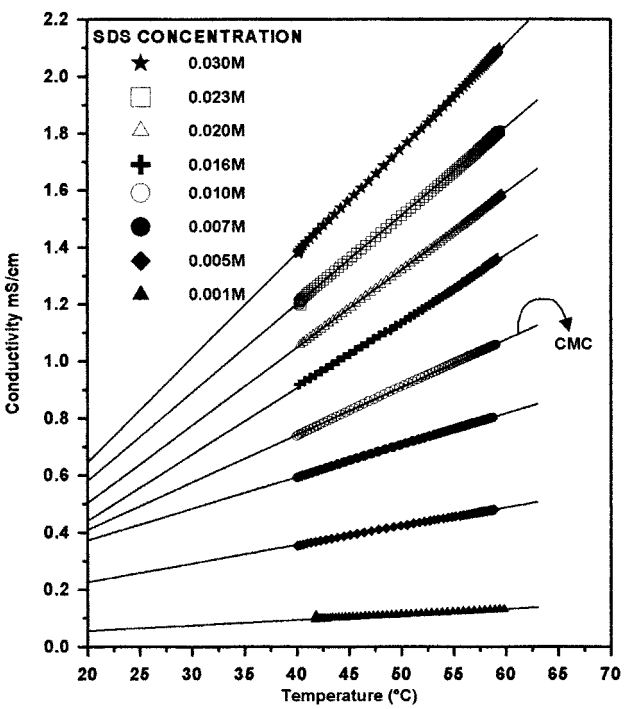

Figure 2 Conductivity measurements of SDS solutions at various temperatures.

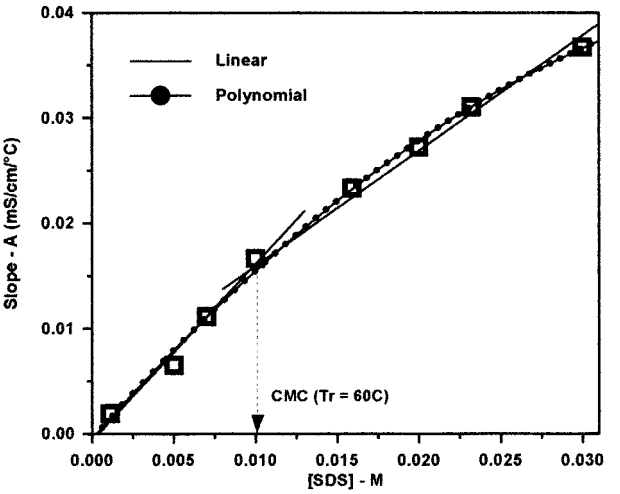

Figure 3 Correlation between slope *A* and the SDS concentration: linear and polynomial fits.

the sensitivity to temperature changes increases as the SDS concentration increases.

This last figure shows that both the angular (slope, or effect of temperature) and linear (effect of SDS) coefficients of the conductivity measurements depend on the SDS concentration. Therefore, temperature corrections must take the SDS concentration into account. However, because the solubility of SDS in water (i.e., the cmc) is also influenced by the temperature, such corrections become a relatively complex task. Most conductivity meters are equipped with temperature measurement devices that perform corrections on the conductivity signal automatically by taking an internal calibration curve based on the conductivity of a KCl standard solution. This approach may be regarded as an approximation because actual conductivity corrections should be carried out with the SDS moving slopes.

A simple inspection of Figure 2 suggests a straightforward correlation between the curve of the slope and the respective SDS concentration. The slope can be described in terms of the SDS concentration, according to Figure 3. As one can verify, the temperature effect can accurately be related to the SDS concentration by either two straight lines or a quadratic curve, covering concentrations below the cmc and well above the cmc. In this case, the use of a quadratic curve instead of two straight lines may be advantageous because the former approach involves fewer parameters (three parameters, instead of four for two straight lines); moreover, the quadratic curve is continuous in the range of SDS concentrations under study.

On the basis of the aforementioned results, one is able to make suitable corrections to the conductivity and to predict the actual surfactant concentrations in aqueous solutions with conductivity and temperature measurements, this being the real interest here. This is

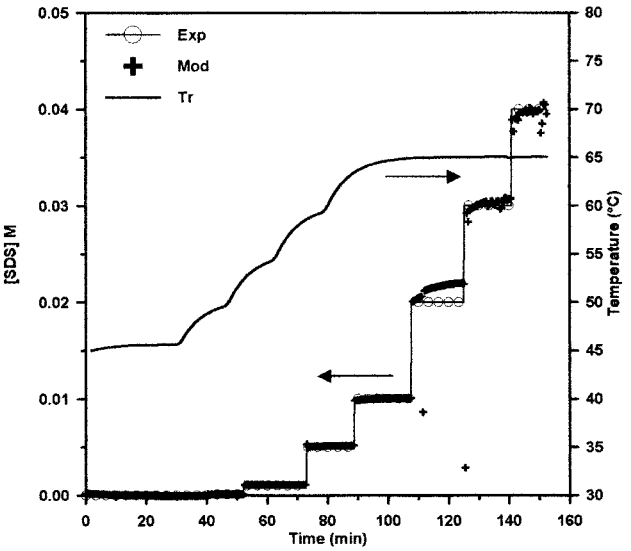

Figure 4 Online monitoring of the SDS concentration (in aqueous media): experimental data, model predictions, and solution temperatures in the reactor (T_r).

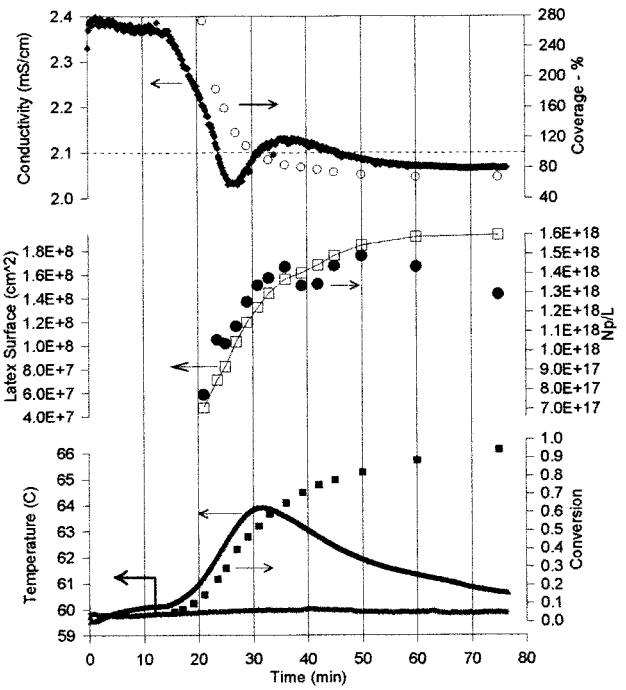

Figure 5 Online monitoring of the conductivity and temperature and offline measurements of the surface coverage, conversion, N_p, and S_L (SDS concentration = 3 × cmc).

illustrated in Figure 4, in which the surfactant concentration is followed during the stepwise addition of SDS into the reactor under heating.

CONDUCTIVITY MEASUREMENTS DURING EMULSION POLYMERIZATIONS

STY polymerization runs are summarized in Table III. The results of the final d_p and θ values are included for each SDS concentration employed in the tests. In this work, the surface coverage was calculated under the assumption that all the surfactant added to the medium was available for particle stabilization. This was done because it is not entirely clear how the surfactant is partitioned between the different phases inside the reactor, especially when tests are carried out with surfactant contents below the cmc. Therefore, values presented here for θ may be regarded as a maximum theoretical value. Computations of the surface coverage were performed according as follows:

$$\theta = \frac{N_{\mathrm{AV}} m_e a_s}{10^{14} S_L \mathrm{MW}_e} \tag{2}$$

TABLE III
STY Emulsion Polymerization Batches

Experiment	[SDS] (M)	Final d_p (nm)	Final θ (%)
R2	0.02	52	45
R3	0.03	51	67
R1	0.04	46	75
R4	0.05	45	93

KPS = 1.0 g/L; T_r = 60°C; solid contents = 10%; cmc of SDS = 0.0083M at 25°C and 0.01M at 60°C.

where N_{AV} and MW_e are Avogadro's number and the molecular weight of the surfactant (288.38 g/mol for SDS), respectively; m_e is the amount of the surfactant (g) used in the recipe, and a_s is equal to 45 Å^2 Typical results for the online monitoring of reaction and jacket temperatures and conductivity during an STY emulsion polymerization batch are shown in Figure 5. Offline data obtained for the conversion, S_L, surface coverage, and N_p are also presented. Initially, the conductivity signal remains constant because of the inhibition period. When the reaction starts, particles are formed, causing an increase in the total particle surface area. The surfactant is, therefore, adsorbed from the aqueous phase onto the newly formed surface, and this leads to a decrease in the conductivity signal. Afterward, the conductivity signal increases, probably because of the monomer consumption in the medium, which can release small amounts of the surfactant into the continuous phase. Finally, when the surface coverage tends to stabilize, the conductivity signal presents a slight decrease that can be associated with the surface area increase, as observed experimentally. The effect of particle shrinkage, if it occurs, may be too small to compensate for the conductivity decrease provoked by the S_L increase observed experimentally.

Surfactant partition modeling

Based on the previous results, a semiempirical mathematical model is proposed for the conductivity sig-

nal, as described in eq. (3). In this case, the conductivity signal is assumed to be the sum of contributions from surfactant molecules present in the latex as free molecules, as micelles, and as adsorbed species. In eq. (3), there is no clear contribution from components other than an ionic surfactant. In a batch reactor under conditions in which the initiator decomposes slowly, the contribution of the persulfates to the conductivity signal is included in a constant baseline (σ_0). Moreover, the form of eq. (3) seems to be supported by the experimental results presented in the previous section for aqueous SDS solutions, with the inclusion of an additional reaction state, which stands for the ratio between the adsorbed mass of the surfactant onto the polymer particles (m_e^{ads}) and the average mass of a single polymer particle (m_p). In fact, this last term implicitly accounts for the S_L effects on the conductivity signal. Besides, it explicitly considers the surfactant partitioning. It should be noted that the amount of the surfactant absorbed by the monomer droplets is assumed to be negligible. However, one may reconsider this assumption when monomer droplets are small enough to provide high surface area, as occurs in miniemulsion and microemulsion polymerizations.

As conductivity is strongly influenced by temperature changes, deviations from the set-point temperature (T_0 = 60°C) are taken into account in the model according to eq. (4):

$$\sigma = \sigma_0 + (\xi_0)\frac{m_e^{\text{aq}}}{V^{\text{aq}}} + (\xi_1)\frac{m_e^{\text{mic}}}{V^{\text{aq}}} + (\xi_2)\left(\frac{1}{m_p}\right)\frac{m_e^{\text{ads}}}{V^{\text{aq}}} \quad (3)$$

$$\begin{bmatrix}\sigma_0\\ \xi_0\\ \xi_1\\ \xi_2\end{bmatrix} = \begin{bmatrix}\hat{\sigma}_0 & \sigma_0^T\\ \hat{\xi}_0 & \xi_0^T\\ \hat{\xi}_1 & \xi_1^T\\ \hat{\xi}_2 & \xi_2^T\end{bmatrix}\begin{bmatrix}1\\ (T_0 - T_r)\end{bmatrix} \quad (4)$$

The determination of surfactant partitioning is the key in eqs. (3) and (4). A simple kinetic model can be used for the computation of monomer partitioning as follows. Equation (5) describes the critical conversion value at which monomer droplets disappear [the appendix shows how eq. (5) is derived]. Therefore, before this critical value, the particle volume and S_L can be computed with eqs. (6a)–(9a). Otherwise, after the depletion of monomer droplets, these variables can be computed with eqs. (6b)–(9b). Equations (7a) and (7b) stand for the polymer particle density (ρ_p), whereas eqs. (8a) and (8b) stand for the single particle volume (v_p). Analogously, eqs. (9a) and (9b) describe the total latex surface area before and after monomer depletion. m_p is given by eq. 10. It is important to note that eqs. (8) and (9) depend on N_p.

It is assumed here that a_s changes slightly with the monomer conversion. This is likely to occur because particles evolve from a monomer-swollen state to a high polymer concentration state, and this leads to changes in the surface polarity. Besides, the hydrophilic characteristics of the aqueous medium can also change significantly during the course of the reaction. Therefore, it is reasonable to assume that the conductivity measurements may be sensitive to the surfactant adsorption–desorption trends, expressed in terms of varying a_s. This is accomplished in the model by the definition of the specific area of the surfactant as a linear function of conversion, as shown in eq. (11). In this case, the linear coefficient term a_{sm} (the maximum specific adsorption area) is assumed to be equal to the reported values (45 Å^2). The angular coefficient a_{sp} can assume either negative values, if the hydrophobic characteristics of the particle increase, or positive values, in the opposite case.

Warson[23] stated that the specific surface could vary as $\ln a_s = k + f(X)$, where k represents a constant and $f(X)$ is a function of the polarity of the polymer surface. Vijayendran[16] used the same expression, also suggesting that the water solubility of organic liquids is a rough measure of polarity. In this sense, we could correlate the specific surface to the monomer concentration in the water phase. Piirma and Chen[20] observed that the measured specific area of SDS onto polystyrene increased with the benzene/polystyrene swelling ratio. In this case, the solvent and the polymer molecules may compete with the surfactant tails for the adsorption surface. The affinity between surfactant molecules is, therefore, reduced, and an increase in the specific area is to be expected. In this sense, we could correlate the specific surface to the monomer concentration in the polymer particles. In conclusion, one can find sufficient arguments to correlate a_s with the monomer concentration either in the water phase or in the polymer particles. However, both correlations seem to be properly resumed on a simple correlation with the monomer conversion:

$$x^* = \frac{\left(\frac{1-\phi^*}{\phi^*}\right)\frac{\rho_{\text{pol}}}{\rho_m}}{1 + \left(\frac{1-\phi^*}{\phi^*}\right)\frac{\rho_{\text{pol}}}{\rho_m}} \quad (5)$$

$$x < x^* \quad (6a)$$

$$x > x^* \quad (6b)$$

$$\rho_p = \phi^*\rho_m + (1-\phi^*)\rho_{\text{pol}} \quad (7a)$$

$$\rho_p = \frac{1}{\frac{x}{\rho_{\text{pol}}} + \frac{(1-x)}{\rho_m}} \quad (7b)$$

$$v_p = \frac{m_m x}{\rho_{\text{pol}} N_p (1-\phi^*)} \quad (8a)$$

TABLE IV
Physical Constants used for Model Building

Constant		Reference
ρ_{pol} (g/cm^3)	1.05	9
ρ_m (g/cm^3)	$-\left(1+\left(1-\frac{[T_r+273]}{C_3}\right)^{C_4}\right)=\frac{MW_m}{1000}C_1C_2$	25
	Styrene $\cdots$ $C_1 = 0.7397$; $C_2 = 0.2603$; $C_3 = 636$; $C_4 = 0.3009$	
MW_m (g/gmol)	104.12	9
a_{sm} (Å^2)	45 (SDS/polystyrene)	This work
cmc (g/L)	3.0 (SDS)	This work

$$v_p = \frac{m_m}{\rho_p N_p} \tag{8b}$$

$$S_L = (36\pi)^{1/3}\left(\frac{N_p(m_m x)^2}{\rho_{pol}^2(1-\phi^*)^2}\right)^{1/3} \tag{9a}$$

$$S_L = (36\pi)^{1/3}\left(\frac{N_p m_m^2(x\rho_m + (1-x)\rho_{pol})^2}{\rho_m\rho_{pol}}\right)^{1/3} \tag{9b}$$

$$m_p = \rho_p v_p \tag{10}$$

$$a_s = a_{sm} + a_{sp}(x) \tag{11}$$

$$m_e^{ads} = \frac{S_L MW_e}{a_s Na} \tag{12}$$

$$m_e^{aq} = V^{aq}cmc \tag{13}$$

$$m_e^{mic} = m_e - m_e^{ads} - m_e^{aq} \tag{14}$$

If m_e^{mic} is less than 0,

$$m_e^{ads} = \frac{S_L MW_e}{a_s N_{AV}}\left(\frac{K_{eq}S_L}{1+K_{eq}S_L}\right) \tag{15}$$

$$m_e^{aq} = m_e - m_e^{ads} \tag{16}$$

On the basis of the previous definitions, surfactant partitioning can be described by eqs. (12)–(16) according to the mass balance of the surfactant species. It is assumed that surfactant species can be adsorbed onto particles, dissolved as free molecules in the aqueous phase, and organized as micelles. A modified Langmuir isotherm is used to describe surfactant adsorption phenomena when micelles are not present, depending on an equilibrium constant (K_{eq}) that may be estimated. Giannetti[22] stated that the SDS desorption from polystyrene particles is a very slow process, reporting $K_{eq} = 7.58 \times 10^{-6}$ (at 50°C).

Parameter estimation

Assuming that data for conductivity, monomer conversion, N_p, temperature, initial loads of chemical species, and polymer/monomer densities are known, we can estimate the parameters of eqs. (3) and (4) for each polymerization batch reported in Table III. The optimization procedure used here is based on a maximum likelihood method described elsewhere.[24]

During the parameter estimation tests, the conductivity signal was taken as the output variable. Besides the parameters of eqs. (3) and (4), the critical monomer volume fraction in the particle (ϕ^*), a_{sp}, and K_{eq} were also fine-tuned. The optimization results for each polymerization batch are summarized in the following figures. The remaining physical constants required for simulations and used in all tests are reported in Table IV. The parameter estimates and the respective 95% confidence intervals are shown in Table V.

Figure 6 compares model predictions and experimental data for the conductivity signals for R2, R3, R1, and R4. It can be verified that the model provides very good fits of the experimental values for all tests. Moreover, the obtained model parameters present small errors (Table V), with the exception of K_{eq} in R2 and R4. As shown by Immanuel et al.,[26] Morbidelli et al.,[27] and Saldivar et al.,[28] this is not unusual and should not be overemphasized.

The parameters summarized in Table V differ from batch to batch, but in most cases, model parameters tend to increase or decrease monotonically as a function of the surfactant concentration. For this reason, regression tests were performed to investigate whether the parameters could be correlated to the SDS concentration.

As shown in Figure 7, each of the model parameters in the conductivity model can be empirically related to the overall SDS concentration in the recipe through simple parabolic or linear fits, as also observed previously for the aqueous SDS solutions. These results encourage the implementation of a more general model structure, with a single set of model parameters for all batches, taking the overall SDS concentration in the recipe into account. In this case, the model takes the form of eq. (17):

TABLE V
Estimated Parameters and 95% Confidence Intervals for Single Batches

Parameter	Estimates ± 2STD			
	SDS = 0.02*M* (R2)	SDS = 0.03*M* (R3)	SDS = 0.04*M* (R1)	SDS = 0.05*M* (R4)
$\hat{\sigma}_0$	1.6296 ± 0.0030	2.0102 ± 0.0011	2.4021 ± 0.0078	2.6066 ± 0.0162
σ_0^T	0.0212 ± 0.0048	0.0120 ± 0.0005	−0.0146 ± 0.0020	−0.0849 ± 0.0111
$\hat{\xi}_0$	−0.0326 ± 0.0013	−0.0021 ± 0.0004	0.1346 ± 0.0101	0.1409 ± 0.0089
ξ_0^T	0.0067 ± 0.0006	0.0090 ± 0.0013	0.0252 ± 0.0017	0.0349 ± 0.0012
$\hat{\xi}_1$	0.2295 ± 0.0241	0.0900 ± 0.0028	0.0048 ± 0.0056	−0.0134 ± 0.0031
ξ_1^T	0.0041 ± 0.0008	0.0040 ± 0.0024	0.0122 ± 0.0005	0.0076 ± 0.0008
$\hat{\xi}_2$	0.0128 ± 0.0008	0.0080 ± 0.0009	0.0055 ± 0.0007	−0.0017 ± 0.0009
ξ_2^T	−0.0044 ± 0.0005	−0.0016 ± 0.0001	−0.0003 ± 0.0002	0.0028 ± 0.0006
ϕ^*	0.1274 ± 0.0134	0.1300 ± 0.0267	0.1000 ± 0.0000	0.1205 ± 0.0074
θ_p	−7.92 ± 1.53	−18.00 ± 2.54	−14.86 ± 0.29	−12.32 ± 0.45
K_{eq}	$2.7 \times 10^5 \pm 5.4 \times 10^5$	$1.0 \times 10^5 \pm 1.0 \times 10^7$	$1.0 \times 10^5 \pm 1.0 \times 10^7$	$1.98 \times 10^4 \pm 1.1 \times 10^2$

$$\begin{bmatrix} \sigma_0 \\ \xi_0 \\ \xi_1 \\ \xi_2 \end{bmatrix} = \begin{bmatrix} \hat{\sigma}_0 & \sigma_0^T & \sigma_0^E & \sigma_0^{ET} & \sigma_0^{EE} & \sigma_0^{EET} \\ \hat{\xi}_0 & \xi_0^T & \xi_0^E & \xi_0^{ET} & \xi_0^{EE} & 0 \\ \hat{\xi}_1 & \xi_1^T & \xi_1^E & \xi_1^{ET} & \xi_1^{EE} & \xi_1^{EET} \\ \hat{\xi}_2 & \xi_2^T & \xi_2^E & \xi_2^{ET} & \xi_2^{EE} & 0 \end{bmatrix} \begin{bmatrix} 1 \\ (T_0 - T_r) \\ [\text{SDS}] \\ (T_0 - T_r)[\text{SDS}] \\ C_e^2 \\ (T_0 - T_r)[\text{SDS}]^2 \end{bmatrix} \quad (17)$$

Besides the temperature, it is also supposed that model parameters are influenced by the ionic strength of the medium, which may be related to the different sodium ion concentrations (the surfactant counterion) used in each particular polymerization recipe. The initiator effect on the ionic strength is not considered because the initiator concentration is small and because it is kept constant in the recipes. One may wonder whether or not the number of parameters involved in eq. (17) is too large. These parameters were selected to link the different batches, and the structure of the semiempirical model proposed here was chosen on the basis of experimental evidence that demonstrated a certain number of functional variations of the parameters contributing to the overall conductivity signal. We are aware that the high number of model parameters in the set can be dangerous and limit the applicability of the model. This will be tested later in this article and in a follow-up article. It should also be pointed out that the number of parameters normally used to build a neural network model is even greater.[21] Additionally, neural networks are black-box models with parameters that cannot be interpreted in physical terms. However, the conductivity model given by eq. (3) is quite simple and takes into account

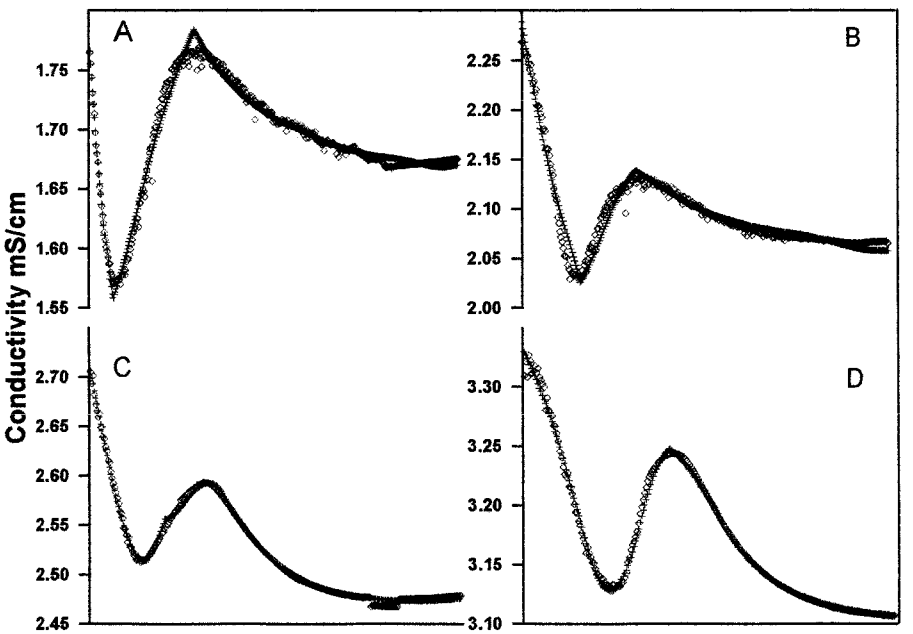

Figure 6 (◇) Experimental and (+) predicted conductivity signals: (A) R2, (B) R3, (C) R1, and (D) R4.

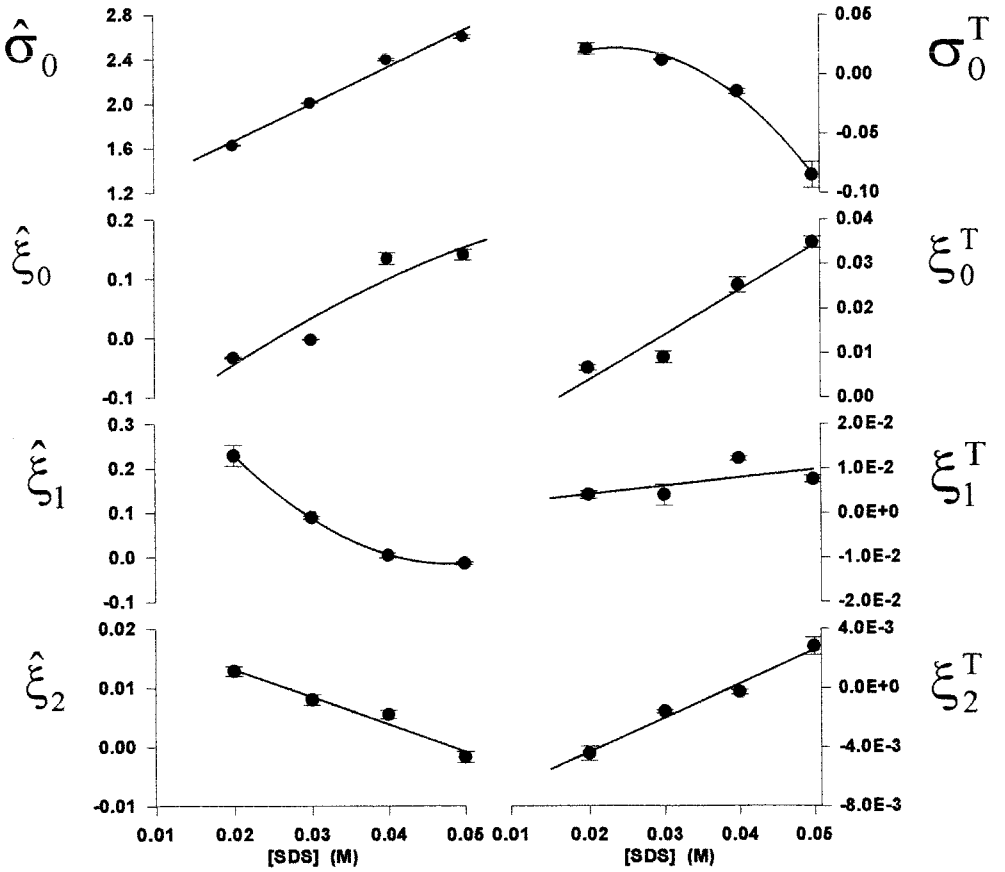

Figure 7 Regression tests between the estimated parameters and SDS concentrations in the recipes.

the individual contributions of the surfactant concentrations in the different phases. The need to enlarge the parameter space is due to the possibility of encountering nonnegligible drifts in temperature and ionic strength and the need to include these when the conductivity response is interpreted. However, special attention must definitely be paid to avoid overfitting the calibration experimental data. Validation tests should also be performed to verify whether or not the model is able to capture the surfactant dynamics in the latex under different conditions. It must be stressed, however, that the effects included in eq. (17) are the same effects observed previously for simple aqueous SDS solutions.

Table VI summarizes the set of parameter estimates for the entire data set (runs R1–R4). The parameter estimates exhibit very small errors, with the exception of $\hat{\xi}_1$, which is related to the micelle concentration. This suggests that the micelle concentration may be a bit more uncertain. A small negative value was found for a_{sp}. a_{sm} was set at 50 Å^2, which is similar to the values reported in the literature. Then, the resulting SDS specific adsorption area can vary from 50 to 48.7 Å^2 during reactions. K_{eq} is also well estimated, with a value comparable to that obtained by Giannetti.[22]

A comparison between the experimental conductivity signal and the model predictions can be seen in Figure 8. The results show very good agreement between experimental data and model predictions and encourage the determination of latex properties on the basis of conductivity measurements. The model derived here is able to predict conductivity data when the conversion, total SDS, temperature, and N_p are known, according to the scheme displayed in Figure 9. It should, therefore, be possible to predict N_p during an actual operation if one combines the model with the available conductivity signal, conversion, and temperature measurements. In this case, the model should be inverted to allow for the determination of the surfactant concentration in the many phases and N_p.

MODEL INVERSION FOR MONITORING N_P

As N_p does not appear explicitly in the model, it is necessary to solve the model iteratively. For simplicity, a direct search method was selected (Golden section method[29]) according to the algorithm depicted in the appendix. This is one of the simplest methods for finding a root of an equation. One of its main drawbacks is the need for two initial guesses, which bracket the root. A search interval is chosen, and the conductivity model is evaluated for two initial guesses of N_p. The resulting model output is then compared to the experimental value of conductivity. Sequential model

TABLE VI
Estimated Model Parameters and 95% Confidence Intervals for the General Model

Parameter	Estimate ± 2STD	Units
$\hat{\sigma}_0$	0.4090 ± 0.0371	mS/cm
σ_0^T	−0.3265 ± 0.0138	mS/cm/°C
σ_0^E	130.57 ± 4.19	(mS/cm)/(g/L)
σ_0^{ET}	19.14 ± 1.29	(mS/cm)/(g/L)/°C
σ_0^{EE}	$-2.49 \times 10^4 \pm 1.60 \times 10^3$	(mS/cm)/(g/L)^2
σ_0^{EET}	372.42 ± 25.21	(mS/cm)/(g/L)^2/°C
$\hat{\xi}_0$	0.1111 ± 0.0072	(mS/cm)/(g/L)
ξ_0^T	0.0463 ± 0.0036	(mS/cm)/(g/L)/°C
ξ_0^E	−9.94 ± 0.67	(mS/cm)/(g/L)^2
ξ_0^{ET}	0.1978 ± 0.0949	(mS/cm)/(g/L)^2/°C
ξ_0^{EE}	348.96 ± 13.72	(mS/cm)/(g/L)^3
$\hat{\xi}_1$	−0.0168 ± 0.0265	(mS/cm)/(g/L)
ξ_1^T	−0.0618 ± 0.0266	(mS/cm)/(g/L)/°C
ξ_1^E	−3.771 ± 1.329	(mS/cm)/(g/L)^2
ξ_1^{ET}	3.619 ± 1.236	(mS/cm)/(g/L)^2/°C
ξ_1^{EE}	$-2.22 \times 10^3 \pm 8.66 \times 10^2$	(mS/cm)/(g/L)^3
ξ_1^{EET}	39.3339 ± 14.1925	(mS/cm)/(g/L)^3/°C
$\hat{\xi}_2$	−0.4953 ± 0.0141	1 · (mS/cm)
ξ_2^T	0.0116 ± 0.0021	1 · (mS/cm)/°C
ξ_2^E	24.4 ± 0.7	1 · (mS/cm)/(g/L)
ξ_2^{ET}	−0.0830 ± 0.0493	1 · (mS/cm)/(g/L)/°C
ξ_2^{EE}	−255.28 ± 7.20	(mS/cm)/(g/L)^3
ϕ^*	0.332 ± 0.003	—
a_{sp}	−1.26 ± 0.14	Å^2
a_{sm}	50.0	Å^2
K_{eq}	$1.0 \times 10^6 \pm 1.0 \times 10^7$	1/cm^2

evaluations are performed, and the N_p value that provides the lowest difference between experimental and predicted conductivity is kept for the next model evaluation. The other N_p value is then eliminated, and this leads to a narrower search interval. This interval elimination is repeated until either the exact root has been found or the interval is smaller than some specified tolerance.

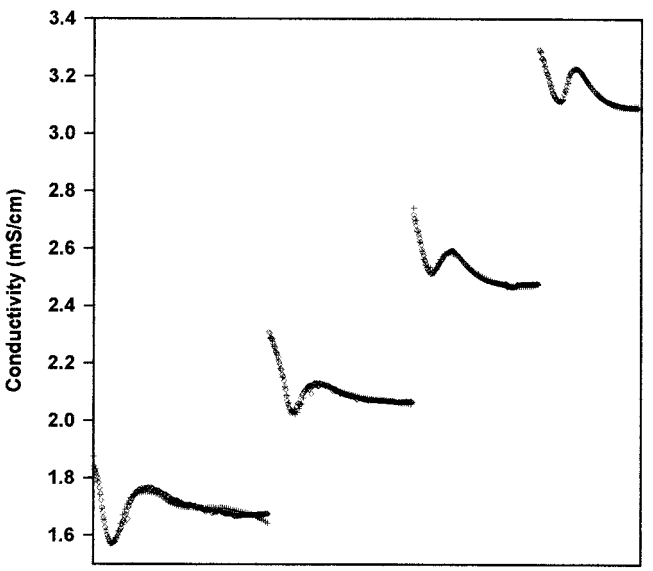

Figure 8 (◇) Experimental and (+) predicted conductivity signals: calibration for the whole data set.

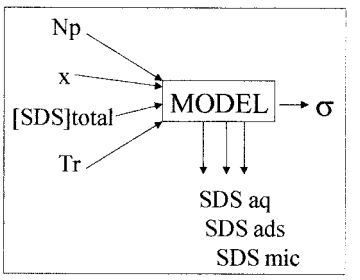

Figure 9. Conductivity model scheme relating input and output variables during calibration tests.

When the iterative procedure is finished, one also obtains estimates of the surfactant partitioning among the many phases, as illustrated in Figure 10. Such a strategy can be applied either online or offline; this depends on whether the temperature and conversion measurement devices are available or not.

Figure 11 shows results obtained when the conductivity model is inverted for reactions R1–R4. Estimates of N_p are compared with experimental values. Model estimates for surfactant partitioning in the phases and offline measurements of the conversion and surface coverage for the different runs are also presented, with dashed lines indicating 100% experimental surface coverage.

Model predictions presented in Figure 11 for N_p are in very good agreement with experimental data in all the tests. The direct search method applied was able to provide reliable N_p values, even when the conductivity signal was disturbed, as in reaction R1. When the total surfactant concentration is low, the model predicts that all the surfactant is adsorbed onto the particle surfaces at the end of the batch. When the surfactant concentration is large, as in R4, the model predicts the existence of micelles in the final latex. For the purpose of N_p monitoring, the results may be regarded as extremely good and show the proper filtering of noisy experimental N_p data.

Although one may be tempted to think that results presented in Figure 11 are not very significant, as the experimental data were used for model calibration, one should also consider the following additional aspects. First, the model was calibrated for conductivity data and not for polymer particle concentration data. Second, model inversion is not guaranteed to work, as

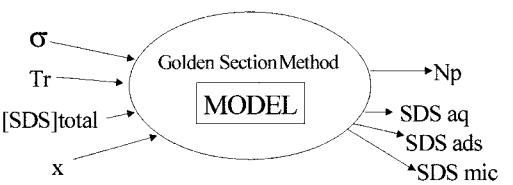

Figure 10 N_p prediction strategy through the conductivity model and online measurements.

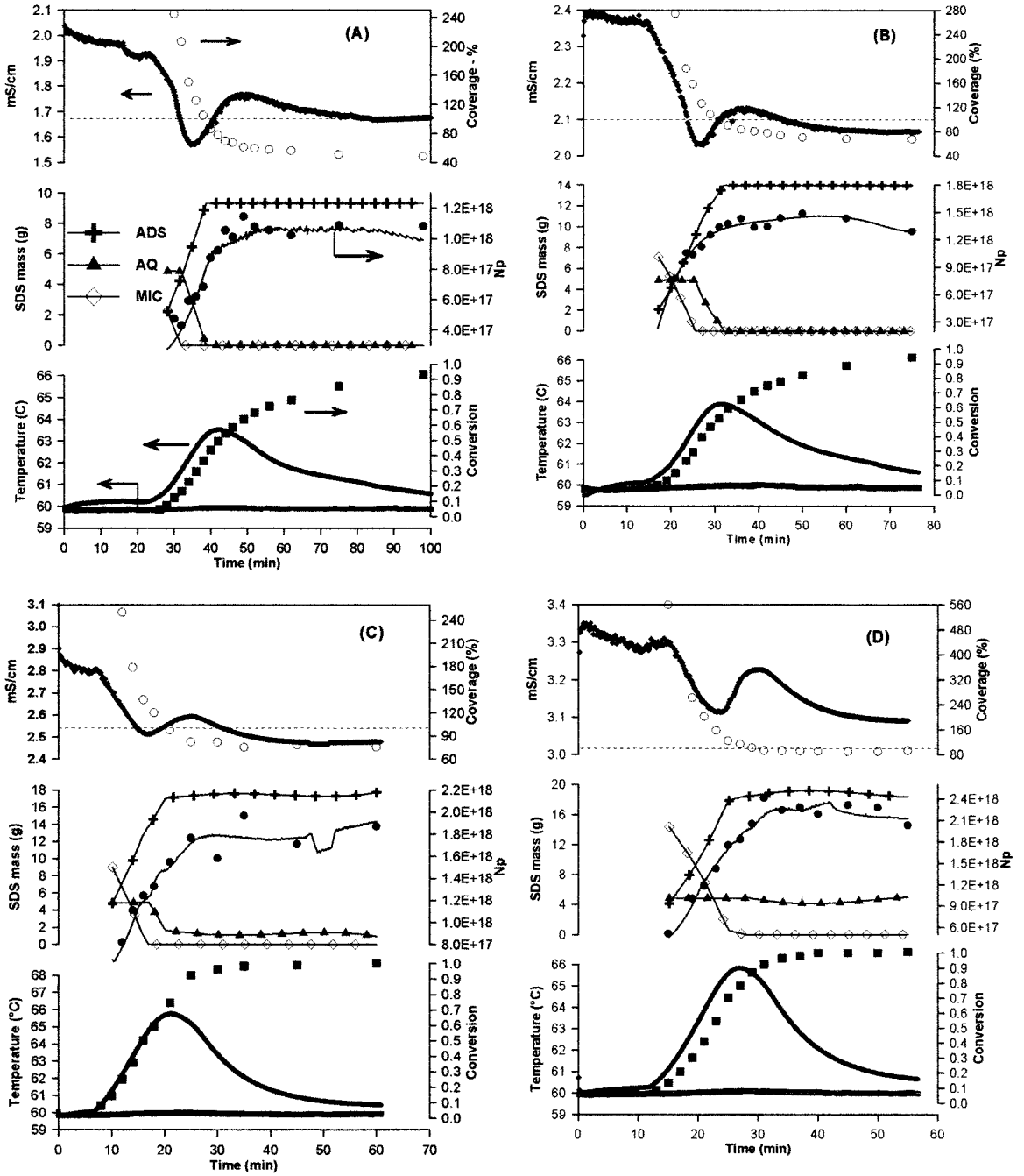

Figure 11 Experimental offline latex properties, online measurements, and model results for N_p and surfactant masses in the phases (parts A–D correspond to 2, 3, 4, 5 × cmc) respectively.

experimental noise can be amplified in certain situations. Besides, depending on the model structure, model inversion could be impossible. Finally, detailed data for surfactant partitioning were not presented for model calibration. Therefore, the obtained results are encouraging. As further proof of the validity of this model, Figure 12 shows model inversion results for two additional experimental runs, S5 and S13 (Table VII), not used during the model development. It should be emphasized that the model was able to perform good predictions, even though S13 was carried out with a 20% solid content in the recipe.

CONCLUSIONS

During emulsion polymerization runs, the use of online conductivity data has been limited to the qualitative description of emulsion polymerization processes and to the identification of kinetic intervals. One of the reasons for these limitations is that the exact nature of

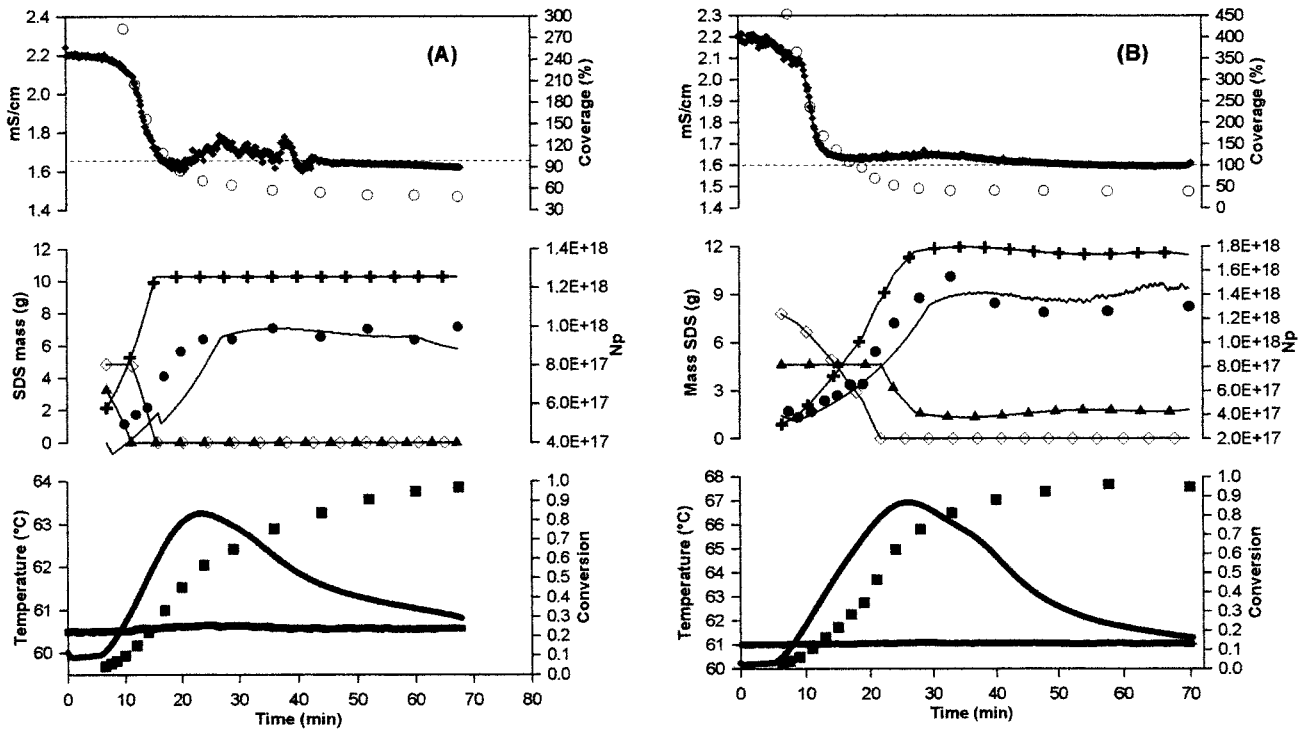

Figure 12 Experimental offline latex properties, online measurements, and model results for N_p and surfactant masses in the phases: validation results for (A) S5 and (B) S13.

all the factors that determine the conductivity signal is still not totally clear. In this study, a conductivity meter was combined with a calorimetric reactor to provide *in situ* and online measurements of conductivity during the emulsion polymerization of STY, with SDS as an anionic surfactant. It has been shown that a semiempirical model can be built to describe the conductivity signal as a function of the latex composition and the reactor temperature. The model was inverted and combined with the available conductivity signal, conversion, and temperature measurements and was able to accurately predict N_p and the surfactant concentration in the many phases, without online measurements of the particle size, even when different solid contents were employed in the experiments. Therefore, interesting control applications can be found by the combined use of the conductimetric model and the online measurements of temperature, monomer conversion, and conductivity data during emulsion polymerization processes. The extension of this model to moderately high solid content systems and semibatch polymerizations will be discussed in part II of this series.

TABLE VII
STY Emulsion Polymerization Validation Experiments

Experiment	[SDS] (M)	Final d_p (nm)	Final θ (%)	Solid content (%)
S5	0.02	57	48	10
S13	0.03	65	38	20

KPS = 1.0 g/L; T_r = 60°C.

This work was carried out as a part of a Brazil–France Cooperation CAPES (Coordenação de Aperfeiçoamento de Pessoal de Nível Superior)/ COFECUB (Comité Français d'Evaluation de la Coopération Universitaire avec le Brésil) project. J.C.P. thanks Fundação de Amparo à Pesquisa do Estado do Rio de Janeiro and Conselho Nacional de Desenvolvimento Científico e Tecnológico for supporting this work and providing scholarships.

APPENDIX

The monomer balance in the emulsion polymerization reactor can be described as follows:

$$m_m(1 - x) = m_m^d + m_m^{aq} + m_m^p \tag{A.1}$$

The monomer volume fraction in the particle (ϕ) can be written, in general, as follows:

$$\phi = \frac{\dfrac{m_m^p}{\rho_m}}{\dfrac{m_m^p}{\rho_m} + \dfrac{m_{pol}}{\rho_{pol}}} \tag{A.2}$$

Calculating the polymer volume and inserting eq. (A.1) into eq. (A.2), we obtain the following:

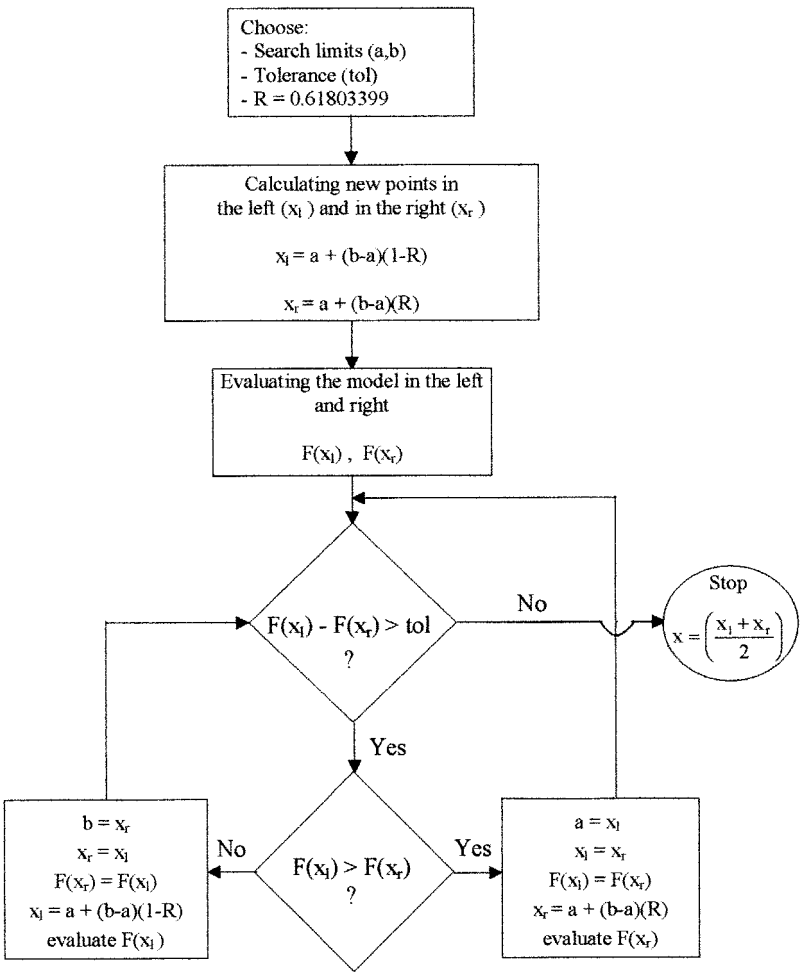

Figure A.1 Golden section method algorithm.

$$\phi = \frac{\dfrac{m_m(1-x) - m_m^d - m_m^{aq}}{\rho_m}}{\dfrac{m_m(1-x) - m_m^d - m_m^{aq}}{\rho_m} + \dfrac{m_m x}{\rho_{pol}}} \qquad (A.3)$$

As a good approximation for STY, the monomer content in the aqueous phase is assumed to be negligible. Computing ϕ^*, the monomer volume fraction in the particles when monomer droplets disappear, we obtain the following:

$$\phi^* = \frac{\dfrac{(1-x^*)}{\rho_m}}{\dfrac{(1-x^*)}{\rho_m} + \dfrac{x^*}{\rho_{pol}}} \qquad (A.4)$$

Finally, eq. (5) can be obtained by the rearrangement of eq. (A.4) in terms of the critical conversion (x^*).

N_p and S_L, experimentally computed in the laboratory, are given by the following equations:

$$N_p = \frac{6 m_m x 10^{21}}{\pi \rho_{pol} d_p^3} \qquad (A.5)$$

$$S_L = \frac{N_p \pi d_p^2}{10^{14}} \qquad (A.6)$$

Figure A.1 illustrates the Golden section algorithm used in the model inversion calculations.

NOMENCLATURE

Abbreviations

a_s	specific area occupied by a surfactant molecule over a polymer particle (Å^2)
cmc	critical micelle concentration (g/L)
d_p	particle diameter (nm)
[DS^-]	concentration of the dodecyl sulfate ion (mol/cm^3)
$f(X)$	function of the polarity of the polymer surface

k constant
K_{eq} equilibrium constant
KPS potassium persulfate
MMA methyl methacrylate
m_e total mass of the surfactant added to the reactor (g)
m_m total mass of the monomer added to the reactor (g)
m_p mass of a single polymer particle (g)
MW_e molecular weight of the surfactant (g/mol)
$[Na^+]$ concentration of the sodium ion (mol/cm^3)
N_{AV} Avogadro's number (molecules/mol)
N_p number of particles in the latex
SDS sodium dodecyl sulfate
S_L latex surface area (cm^2)
STD standard deviation of parameter estimates
STY styrene
T_0 set-point temperature (°C)
T_r reaction temperature (°C)
V volume (L)
v_p single particle volume
x conversion
X polarity of the polymer surface
x^* conversion at which monomer droplets disappear

Greek letters

θ surface coverage by the surfactant (%)
$\Lambda_0^{\,i}$ equivalent ionic conductivity at infinite dilution of ion i (cm^2 S/mol)
ξ_i conductivity model parameters (i = 0, 1, or 2)
ρ density (g/cm^3)
ρ_p polymer particle density (g/cm^3)
σ total conductivity (S/cm)
σ_0 conductivity contribution from all other ions present in the water (S/cm)
τ solid content (%)
ϕ monomer volume fraction in the particle
ϕ^* critical monomer volume fraction in the particle

Subscripts and superscripts

aq aqueous phase
ads adsorbed species
d monomer droplet phase
e emulsifier or surfactant
E gain term linked to the emulsifier (see the model parameters)
m monomer
mic micelles
p particle
pol polymer
T gain term linked to the temperature (see the model parameters)
* saturation or critical value at the interval II–III transition

References

1. El-Aasser, M. S.; Sudol, E. D. In Emulsion Polymerization and Emulsion Polymers; Lovell, P. A.; El-Aasser, M. S., Eds.; Wiley: Chichester, England, 1997; p 38.
2. Dimitratos, J.; Eliçabe, G.; Georgakis, C. AIChE J 1994, 40, 1993.
3. Flores-Cerrillo, J.; MacGregor, J. F. Ind Eng Chem Res 2002, 41, 1805.
4. (a) Bury, M.; Gerhards, J.; Erni, W. Int J Pharm 1991, 76, 207; (b) Gan, L. M.; Liu, J.; Poon, L. P.; Chew, H. C.; Gan, L. H. Polymer 1997, 38, 5339.
5. Janssen, R. Q. F. Ph.D. Thesis, Eindhoven University of Technology, 1994.
6. Fontenot, K.; Schork, F. J. J Appl Polym Sci 1993, 49, 633.
7. Reimers, J. L.; Schork, F. J. J Appl Polym Sci 1996, 60, 251.
8. Noel, L. J. F.; Janssen, R. Q. F.; van Well, W. J. M.; van Herk, A. M.; German, A. L. J Colloid Interface Sci 1995, 175, 461.
9. Brandrup, J.; Immergut, E. H.; Grulke, E. A. Polymer Handbook, 4th ed.; Wiley: New York, 1999; Chapter 1, p 1.
10. Ruckenstein, E.; Nagarajan, R. J Phys Chem 1975, 79, 2622.
11. Stubbs, J. M.; Durant, Y. G.; Sundberg, D. C. Langmuir 1999, 15, 3250.
12. Shah, S. S.; Saeed, A.; Sharif, Q. M. Colloids Surf A 1999, 155, 405.
13. Desroches, T. Ph.D. Thesis, Université Claude Bernard-Lyon I, 1990.
14. Mokus, M. Ph.D. Thesis, Université Pierre et Marie Curie, 1996.
15. Chen, L.-J.; Lin, S.-Y.; Chern, C.-S.; Wu, S.-C. Colloids Surf A 1997, 122, 161.
16. Vijayendran, B. R. J Appl Polym Sci 1979, 23, 733.
17. Rosen, M. J. Surfactants and Interfacial Phenomena, 2nd ed.; Wiley: New York, 1989.
18. Pérez-Rodriguez, M.; Varela, L. M.; García, M.; Mosquera, V.; Sarmiento, F. J Chem Eng Data 1999, 44, 944.
19. Miyamoto, S.; Tagawa, M. Colloid Polym Sci 1988, 266, 1126.
20. Piirma, I.; Chen, S.-R. J Colloid Interface Sci 1980, 74, 90.
21. Pollard, I. F.; Broussard, M. R.; Garrison, D. B.; San, K. Y. Comput Chem Eng 1992, 16, 253.
22. Giannetti, E. AIChE J 1993, 39, 1210.
23. Warson, H. In Applications of Synthetic Resin Latices; Warson, H.; Finch, C. A., Eds.; Wiley: Chichester, England, 2001; Vol. 1, p 192.
24. Bard, Y. Nonlinear Parameter Estimation; Academic: New York, 1974.
25. Perry's Chemical Engineers' Handbook, 7th ed.; Perry, R. H.; Green, D. W., Eds.; McGraw-Hill: New York, 1997.
26. Immanuel, C. D.; Doyle, F. J., III; Cordeiro, C. F. Dechema Monogr 2001, 137, 313.
27. Morbidelli, M.; Storti, G.; Carra, S. J Appl Polym Sci 1983, 28, 901.
28. Saldivar, E.; Dafniotis, P.; Ray, W. H. J Macromol Sci Rev Macromol Chem Phys 1998, 38, 207.
29. Vanderplaats, G. N. Numerical Optimization Techniques for Engineering Design; McGraw-Hill: New York, 1984.